Spatial and temporal variability of carbonaceous aerosols: assessing the impact of biomass burning in the urban environment

Titos G.[1,2], del Águila A.[1], Cazorla A.[1,3], Lyamani H.[1], Casquero-Vera J.A.[1,3], C. Colombi[4], E. Cuccia[4], V. Gianelle[4], Močnik G.[5,6], Alastuey A.[2], Olmo F.J.[1,3], Alados-Arboledas L.[1,3]

[1]Andalusian Institute for Earth System Research, IISTA-CEAMA, University of Granada, Junta de Andalucía, Granada 18006, Spain

[2] Institute of Environmental Assessment and Water Research (IDÆA), Department of Geosciences, CSIC, Barcelona, Spain.

[3] Department of Applied Physics, University of Granada, Granada 18071, Spain

[4]ARPA Lombardia, Settore Monitoraggi Ambientali, Milano, 20124, Italy

[5]Aerosol d.o.o. Research and Development Department, Ljubljana, Slovenia

[6]Department of Condensed Matter, Jozef Stefan Institute, Ljubljana, Slovenia

Correspondence to:

Gloria Titos Vela

Institute of Environmental Assessment and Water Research (IDÆA), Department of Geosciences, CSIC, Barcelona, Spain

email: gloria.titos@idaea.csic.es

Abstract

Biomass burning (BB) is a significant source of atmospheric particles in many parts of the world. Whereas many studies have demonstrated the importance of BB emissions in central and northern Europe, especially in rural areas, its impact in urban air quality of southern European countries has been sparsely investigated. In this study, highly time resolved multi-wavelength absorption coefficients together with levoglucosan (BB tracer) mass concentrations were combined to apportion carbonaceous aerosol sources. The Aethalometer model takes advantage of the different spectral behaviour of BB and fossil fuel (FF) combustion aerosols. The model was found to be more sensitive to the assumed value of the aerosol Ångström exponent (AAE) for FF (AAE_{ff}) than to the AAE for BB (AAE_{bb}). As result of various sensitivity tests the model was optimized with $AAE_{ff} = 1.1$ and $AAE_{bb} = 2$. The Aethalometer model and levoglucosan tracer estimates were in good agreement. The Aethalometer model was further applied to data from three sites in Granada urban area to evaluate the spatial variation of CM_{ff} and CM_{bb} (carbonaceous matter from FF or BB origin, respectively) concentrations within the city. The results showed that CM_{bb} was lower in the city centre while it has an unexpected profound impact on the CM levels measured in the suburbs (about 40%). Analysis of BB tracers with respect to wind speed suggested that BB was dominated by sources outside the city, to the west in a rural area. Distinguishing whether it corresponds to agricultural waste burning or with biomass burning for domestic heating was not possible. This study also shows that although traffic restrictions measures contribute to reduce carbonaceous concentrations, the extent of the reduction is very local. Other sources such as BB, which can contribute to CM as much as traffic emissions, should be targeted to reduce air pollution.

Keywords: biomass burning, fossil fuel, carbonaceous matter, Aethalometer, Ångström exponent.

1 Introduction

The study of ambient particulate matter (PM) concentrations in urban environments is of interest due to its adverse effects on human health (e.g. Pope and Dockery, 2006). Traffic emissions are of particular concern in urban areas and their surroundings, since traffic-related pollutants have been associated with overall mortality increase (e.g. Hoek et al., 2000), lung cancer risk (e.g. Beelen et al., 2008), and worsening of respiratory health (e.g. Brauer et al., 2002). Among atmospheric pollutants, particulate black carbon (BC) has become a matter of concern during the past years. Black Carbon (BC) is a primary product of incomplete combustion of carbonaceous fuels, normally originated from diesel engines in urban areas (e.g. Hamilton and Mansfield, 1991; Pakkanen et al., 2000). In addition to diesel engines from the traffic sector, biomass burning and domestic heating (based on fossil or biomass fuels) constitute the main sources of BC in the atmosphere. Janssen et al. (2012) reviewed epidemiological, clinical, and toxicological studies and reported sufficient evidence of both short-term and long-term health effects of BC. However, according to these authors, BC itself may not be a major toxic component of PM, but it rather acts as an indicator of other combustion-originating toxic constituents. As stated by the World Health Organization "BC may carry a wide variety of chemicals to the lungs, the body's major defense cells and possibly the circulatory system" (Janssen et al., 2012).

Residential wood burning is an increasingly common popular alternative energy source to fossil fuels since the last years (Fuller et al., 2013). The use of biomass as a heating source has recently increased due to the promotion of CO_2 neutral policies, higher taxes in heating diesel and the financial crisis with significant repercussions on the average household income. In this sense, wood smoke can be an important source of particulate and gaseous pollution significantly affecting rural and urban locations (Viana et al., 2013). This is particularly important during winter when the meteorological conditions in combination with the increase use of biomass burning might significantly and detrimentally impact air quality in urban areas, exposing large populations to pollutant concentrations exceeding regulatory limits. In Central and Northern Europe biomass burning emissions have been identified as a major source of air pollutants (e.g. Yttri et al., 2005; Alfarra et al., 2007; Sandradewi et al., 2008), accounting for up to 80% of fine aerosols (Larssen et al., 2006) and being one of the major sources of organic aerosols (Caseiro et al., 2009) during winter time. In Southern Europe, domestic biomass burning

is a much less frequent practice. However, recent studies conducted in Mediterranean urban areas have identified residential biomass burning as an increasing practice contributing to air quality degradation (Viana et al., 2013; Paraskevopoulou et al., 2015; Sarigiannis et al., 2015; Nava et al., 2015). In addition to biomass burning for residential heating, burning of agricultural waste is a common practice that releases significant amount of gaseous and particulate pollutants into the atmosphere (Andreae and Merlet, 2001; Dambruoso et al., 2014; Kostenidou et al., 2013). For example, Dambruoso et al. (2014) and Kostenidou et al. (2013) showed the large impact of olive tree branches burning on Mediterranean air quality. Farms can be close to densely populated areas, and so, burning of agricultural waste may cause higher exposure to air pollutants increasing potential risks for human health.

Several approaches have been used in the literature to identify biomass burning contribution to aerosolized particulate matter in ambient air. Most of the approaches focus on the determination of chemical biomass burning tracers in PM samples such as water soluble potassium, anhydrosugars like levoglucosan or mannosan, and/or organic carbon (Khalil and Rasmussen, 2003; Alves et al., 2011; Zotter et al., 2016). Other approaches take advantage of the spectral dependence of the absorption coefficient of carbonaceous particles from different sources (Sandradewi et al., 2008; Cazorla et al., 2013; Ealo et al., 2016). Carbonaceous particles from biomass burning sources feature enhanced absorption at shorter wavelengths (Sandradewi et al., 2008). The main advantage of this technique is the availability of real-time online measurements. As a major drawback is important to highlight that other aerosol species like dust may also have an absorption enhancement at shorter wavelengths (Valenzuela et al., 2015).

Atmospheric aerosol optical properties have been widely investigated in the city of Granada at surface level (e.g., Lyamani et al., 2008; Lyamani et al., 2010; Titos et al., 2012; Segura et al., 2014), in the vertical column with height resolution (e.g., Guerrero-Rascado et al., 2008; Alados-Arboledas et al, 2011; Bravo-Aranda et al., 2015 and references therein) and column-integrated (e.g., Lyamani et al., 2005; Valenzuela et al., 2012). The meteorological conditions together with the topography of the city sited in a valley surrounded by mountains of high elevation (about 3500 m a.s.l.) contribute to high concentrations of pollutants close to the surface and their slow dispersion, especially in winter season (Lyamani et al., 2012). Previous studies pointed to traffic as one of the major sources contributing to air quality degradation in Granada; BC mass concentrations

exhibited two distinct maxima during the day in coincidence with traffic rush hours (Lyamani et al., 2011; Titos et al., 2012; Segura et al., 2014). The chemical composition of fine particulate matter (PM_1) during the period 2006–2010 showed that carbonaceous matter (EC+OM) was one of the major contributor to PM_1 at Granada accounting for around 40% of PM_1 and with higher concentrations in winter than in summer (Titos et al., 2014a). OC/EC ratio in Granada is similar to that found in other urban areas in Spain like Madrid or Zaragoza (Querol et al., 2013). Recent research by Titos et al. (2014) identified and apportioned the main aerosol sources of fine and coarse PM in Granada applying the PMF technique (Paatero, 1997) to speciated PM_{10} and PM_1 samples. Traffic exhaust was found to be the major aerosol source contributing around 50% to PM_1 levels during winter (Titos et al., 2014a).

In order to reduce local air pollutants and improve air quality, in the last years local authorities have implemented various measures focusing on reducing traffic emissions, especially in the city centre. These emission abatement measures led to a significant reduction of BC mass concentrations of 37% in the city centre (Titos et al., 2015). However, the efficiency of these measures in the whole urban area was not clear (Titos et al., 2015). Pollutant emissions from other sources such as biomass burning were not included in the emission abatement strategies due to the lack of information on their magnitude and sources. This information is crucial for the implementation of effective mitigation measures. In Andalusia, burning of agricultural residues in the field is allowed during cold season, approximately from 15 October to 1 June (Junta de Andalucía, http://www.juntadeandalucia.es/medioambiente/web/aplicaciones/Normativa/ficheros/O rden%2021_5_09.pdf). The open burning of biomass in combination with the adverse meteorological/synoptic conditions limiting effective dispersion of pollutants during cold season can cause severe air quality problems affecting the Granada urban area. It is important to note that fuel-oil is the main fuel used in domestic heating in Granada: however, in the last years there has been a significant increase in the use of biomass for domestic heating as a result of incentives promoted by the regional government. In fact, the biomass consumption, especially olive pits, has increased from 35-45 ktoe (thousand tons of oil equivalent) before 2009 to 120-150 ktoe after 2009 according to Andalusian energy agency (https://www.agenciaandaluzadelaenergia.es/). Therefore, the identification and quantification of biomass burning contribution to pollutant

concentrations is very important for development of further pollution control strategies in order to improve air quality in Mediterranean urban areas such as Granada.

The main aims of this study are:

- to interpret the temporal and spatial variability of light-absorbing aerosol concentrations and their aerosol absorption spectral dependence over a long study period, and
- to identify other aerosol sources such as biomass burning using multi-wavelength absorption measurements in combination with chemically speciated PM samples.

2. Methodology

2.1 Measurement sites

Granada is located in the Southeastern Iberian Peninsula (37.16° N, 3.61° W, 680 m a.s.l.) and is a non-industrialized city with a population of about 240000 inhabitants and 350000 when including the satellite towns (www.ine.es). The city is situated at the foot of Sierra Nevada Mountains, in a natural valley (see Figure 1). Near-continental conditions are responsible of large temperature variations both seasonally and daily. Long-term aerosol measurements have been performed continuously since 2005 at IISTA-CEAMA (University of Granada, UGR) station which is part of the ACTRIS network and operates under ACTRIS guidelines (http://actris2.nilu.no/). Two additional measurement sites were deployed during one-year period to study aerosol spatial variability within the city of Granada (Figure 1). The three measurement sites are briefly described below:

- **IISTA-CEAMA (UGR)**

The UGR measurement station is located at the IISTA-CEAMA research institute in the southern part of the city of Granada in a pedestrian street with motor traffic about 100 m away. The main highway in the city lies about 470 m away from the station. One of the main arteries of the city, Camino de Ronda, is around 200 m away. Air is sampled from the top of a stainless steel tube of 20 cm diameter and 5 m length located at about 15 m above the ground, on the roof of the building (Lyamani et al., 2008). Due to its location, this station is representative of urban background conditions and as such will be used as a reference site for this study. Measurements at this site reported in this study started in September 2012 and ended on September 2015.

- **Palacio de Congresos (PC)**

This station is part of the Air Quality Network of the Andalusian Regional Government (Consejería de Medio Ambiente, Junta de Andalucía). The station is located close to a children's playground and surrounded by vegetation. The closest road with motor traffic is around 80 m away, where there is a hub for commuting between metropolitan and urban buses. At this site, the inlet is around 4 m above the ground. This air-quality station is considered representative of urban conditions. Measurements at this site lasted from June 2014 to July 2015.

- **Gran Vía (GV)**

The measurement site is located in the city centre. Gran Vía Street is a restricted traffic zone from 7:30 to 22:00 local time, where only buses, motorcycles and authorized cars are allowed to drive. The instrumentation was placed on a balcony facing directly the street. This site can be considered as representative of traffic conditions. Measurements at this site lasted from June 2014 to July 2015.

Figure 1: Map of the city of Granada and surrounding area from Google Earth.

2.2 Measurements and data treatment

Table 1 lists the measurement sites, the instrumentation used and its time resolution and the measurement period.

2.2.1 Aerosol absorption measurements

Aerosol light absorption coefficient, σ_{ap}, was measured at UGR station with a Multi-Angle Absorption Photometer (MAAP, Thermo Scientific model 5012) at 637 nm (Müller et al., 2011). This instrument measures the light transmitted through and backscattered from a particle-loaded filter. The σ_{ap} is calculated using radiative transfer model which includes a treatment of the scattering effects of the filter matrix and the light scattered by the aerosol component. A detailed description of the instrument and method is provided by Petzold and Schönlinner (2004). The MAAP draws the ambient air at constant flow rate of 16.7 l min^{-1} and provides 1 min values. The total method uncertainty for the aerosol light absorption coefficient inferred from MAAP measurements is around 12% (Petzold and Schönlinner, 2004; Petzold et al., 2005).

Table 1: Measurement sites, instrumentation used, time resolution and measurement period for IISTA-CEAMA (UGR), Palacio de Congresos (PC) and Gran Vía (GV) experimental sites.

Measurement site	Instrument	Timebase	Period
UGR	Aethalometer AE31 Aethalometer AE33	2 min 1 min	Sept 2012-June 2014 Jan 2014-Sept 2015
	MAAP	1 min	Sept 2012-Sept 2015
	Weather station High-Vol sampler	1 min 24 h	Sept 2012-Sept 2015 Sept 2012-Sept 2013
PC	Aethalometer AE31	5 min	June 2014-July 2015
GV	Aethalometer AE31	5 min	June 2014-July 2015

Multi-wavelength aerosol light-absorption coefficients were measured at the three experimental sites with Aethalometers (Magee Scientific, Aerosol d.o.o.) at nominal wavelengths of 370, 470, 520, 590, 660, 880 and 950 nm. Two models of Aethalometers were used in this study: AE31 (Hansen and Novakov, 1984) and AE33 (Drinovec et al., 2015). A complete description of the operating principles of Aethalometers can be found in Hansen (2005) and Drinovec et al. (2015). The Aethalometer measures the light attenuation through a quartz filter matrix as aerosols are deposited on the filter. This parameter is defined by

$$ATN(\lambda) = -\ln\left(\frac{I(\lambda)}{I_0(\lambda)}\right) \qquad \text{(Eq. 1)}$$

where I is the intensity of light that passes through the particle-loaded part of the filter, and I_0 is the intensity of light passing through the unloaded part of the filter. The attenuation coefficient (σ_{ATN}) at each wavelength can be obtained by

$$\sigma_{ATN}(\lambda) = \frac{A}{V}\frac{\Delta ATN(\lambda)}{\Delta t} \qquad\qquad\qquad\qquad (Eq.\ 2)$$

where A is the filter spot area, V the flow rate, and ΔATN is the variation in the attenuation measured during the time interval Δt. The flow rate in these instruments was set to 4 l min^{-1}. The time resolution differed between the measurement sites from 1 min (AE33) up to 5 min (AE31), see Table 1.

Filter-based instruments, including the Aethalometers, are subject to different non-linearities. Details on data compensation methodologies can be found for example in Weingartner et al. (2003), Collaud-Coen et al. (2010) and Segura et al. (2014). In this study, Aethalometer measurements were compensated by means of Eq. 3, where C_0 constant is the slope between the attenuation coefficient measured with the Aethalometer and aerosol absorption coefficient obtained by the MAAP.

$$\sigma_{ap}(\lambda) = \frac{\sigma_{ATN}(\lambda)}{C_0} \qquad\qquad\qquad\qquad (Eq.\ 3)$$

For Aethalometers AE31, ACTRIS recommends the use of constant C_0 value of 3.5 assuming a 25% error (Müller et al., ACTRIS-2 WP3 Workshop, November 2015, Athens, Greece). Since at UGR the MAAP was operated side by side with the Aethalometers during an intercomparison period, the specific C_0 constant was calculated for this study. The C_0 values obtained were 1.7±0.4, 3.6±0.9 and 2.7±0.7 for the AE33, AE31 (GV) and AE31 (PC) respectively. By compensating the Aethalometers using these C_0 values we have also accounted for unit-to-unit discrepancies in order to make measurements comparable among sites. Furthermore, Aethalometer data have been screened for negative and extremely high values according to the methodology presented by Segura et al. (2014). Mass equivalent black carbon, EBC, concentrations are determined at 880 nm using a mass absorption cross section (MAC) of 7.77 m^{2}g^{-1} as recommended by the manufacturer. Hereafter we will follow the terminology proposed by Petzold et al. (2013) and we will refer to equivalent black carbon (EBC) since the black carbon data is derived from an optical absorption method.

At UGR, the Aethalometer AE33 was installed next to the AE31 in January 2014, and this AE31 was moved to GV in June 2014. Thus, co-located measurements from January to June 2014 of MAAP and Aethalometers AE31 and AE33 allowed us to assure the comparability and continuity of the measurements at UGR. It is important to note that the

AE31 (GV) and the MAAP used in this study participated in the ACTRIS intercomparison (ACTRIS Intercomparison Workshop for Integrating Nephelometers and Absorption Photometers 2013, Leipzig, Germany) showing good agreement with reference instruments and therefore assuring high quality data for this study. At all measurement sites (UGR, PC and GV) absorption measurements were performed without aerosol size cut-off.

The Absorption Ångström Exponent (AAE) describes the wavelength dependency of the absorption coefficient and it can give information about the predominant aerosol type or source (e.g., Cazorla et al., 2013). In this sense, BC follows a λ^{-1} spectral dependency, yielding an AAE equal to 1 (Bergstrom et al., 2002), and organic carbon and mineral dust have a higher contribution to absorption in the ultraviolet (UV) and blue spectral regions yielding an AAE greater than 1 (Kirchstetter et al., 2004; Valenzuela et al., 2015). AAE has been calculated from the measured absorption coefficients, $\sigma_{ap}(\lambda)$, using Equation 4 for the wavelength pairs 370-520 nm and 370-950 nm.

$$AAE(\lambda_1 - \lambda_2) = -\frac{ln\left(\frac{\sigma_{ap}(\lambda_1)}{\sigma_{ap}(\lambda_2)}\right)}{ln\left(\frac{\lambda_1}{\lambda_2}\right)} \qquad \text{(Eq. 4)}$$

According to results from ACTRIS-2 WP3 (Müller et al., ACTRIS-2 WP3 Workshop, November 2015, Athens, Greece), C_0 constant shows minimal wavelength dependence in the range 470 to 660 nm. However, we observed differences in the AAE retrieved from the different instruments during co-located measurements. Thus, to assure comparability between AAE calculated from different Aethalometers we have referenced the spectral dependence of the AE31 instruments to that of the AE33 which is considered more accurate (Drinovec et al., 2014).

2.2.2 PM$_{10}$ sampling and chemical analysis

24-hour PM$_{10}$ samples (starting at 07:00 GMT) were collected on quartz fiber filters by means of a high-volume sampler (CAV-A/MSb) with a flow rate of 30 m^3 h^{-1} from September 2012 to September 2013. The filters were conditioned and treated pre- and post-sampling. The filters were placed in desiccators during 48 hours at stabilized conditions (23 °C and 50% RH) prior to weighting using gravimetric techniques. A complete chemical analysis was performed for all samples at Institute of Environmental Assessment and Water Research (IDAEA-CSIC, Barcelona, Spain) following the

procedure of Querol et al. (2001). A portion of the filter was used to determine the organic carbon (OC) and elemental carbon (EC) mass concentrations by means of a thermo-optical transmission method using a Sunset Laboratory OCEC Analyser following the EUSAAR2 thermal protocol (Cavalli et al., 2010). The carbonaceous material, CM, was estimated as the sum of organic matter, OM (1.6*OC, Turpin et al., 2000), and elemental carbon, EC. Levoglucosan concentrations were determined from another portion of the filter by ion chromatography with ampherometric detector at ARPA Lombardia (Milan, Italy), following the procedure explained in Vicente et al. (2015).

2.2.3 Ancillary information

Data from a meteorological station located at UGR have been used in this study. Wind velocity and direction were measured by a wind monitor model 05103 (R. M. Young Company). The temperature was recorded by temperature sensor model MTHA1 (ITC) and the relative humidity with a Vaisala sensor. The uncertainty in temperature and relative humidity measurements are 0.4 °C and 1.5%, respectively. The accuracy in wind speed is ±0.3 m/s or 1% of the reading, in the instrument operating range 0-100 m/s. Wind direction is measured with an accuracy of ±3º.

5-days air-mass back trajectories arriving at 00:00, 06:00, 12:00 and 18:00 GMT at Granada at 500 m a.g.l., were computed using the HYSPLIT4 model (Hybrid Single Particle Lagrangian Integrated Trajectory; Draxler et al., 2013) version 4.9 using GDAS meteorological information and were used to support the interpretation of the results. These back-trajectories were clustered using Hysplit 4 software (Draxler et al., 2013). The number of clusters was selected according to the change in the explained variance.

3. Results and discussion

3.1. Temporal variability

The AAE calculated for the ultraviolet-visible range (UV-VIS, 370-520 nm) and for the entire spectral range of the Aethalometers (370-950 nm) were highly correlated (R^2 = 0.84) and exhibited a similar trend (Figure S1 in the Supplementary material). AAE(370-520 nm) was found to be more sensitive to the absorption enhancement at the shortest wavelengths, which enables to identify changes in the spectral dependence more easily. Consequently, the following analysis focuses on the AAE calculated for the 370-520 nm wavelength range. Figure 2 shows the monthly evolution of EBC at 880 nm and AAE

measured at UGR during the 3-years period starting in September 2012. Both variables show a clear seasonal cycle along the studied years, with the largest EBC concentrations and AAE values during winter and the lowest ones during summer. High EBC concentrations during winter are associated with an increase in anthropogenic emissions in combination with lower mixing layer heights (Granados-Muñoz et al., 2012) and frequent stagnant conditions (Lyamani et al., 2012). Large AAE values during winter are related to an increase in the contribution of UV-absorbing particles, likely from biomass burning emissions, since desert dust intrusions over the study area are very scarce during winter (Valenzuela et al., 2012). The sources of these UV-absorbing particles will be analyzed in more detail in the following sections. The standard deviation and interquartile range were also large during winter, denoting high variability in EBC concentrations. Furthermore, changes in the contribution of different absorbing aerosol types are indicated by the large variability observed in AAE values. We attribute this variability to the impact of different sources of absorbing aerosols (i.e., fossil fuel and biomass burning) with a distinct absorption spectral dependence. The EBC seasonality obtained here is in agreement with previous studies performed in Granada using a MAAP for the period 2005-2008 (Lyamani et al., 2008; Lyamani et al., 2010; Lyamani et al., 2011) and in other urban areas (e.g., Viana et al., 2013; Segura et al., 2016).

Slightly lower EBC values were measured in winter 2013/2014 compared to the rest of the analyzed winters. However, no significant change in the AAE was observed, suggesting that absorbing aerosol sources were likely similar from year to year. The decrease in EBC concentration in winter 2013/2014 may be due to a reduction in EBC emissions or change in meteorological conditions or both. We have analyzed the meteorological variables in order to investigate whether the reduction in the EBC in winter 2013/2014 was associated to changes in the meteorological conditions. The results show that temperature, relative humidity, wind speed and direction and precipitation were statistically similar during winters 2012/2013 (November 2012 – February 2013), 2013/2014 (November 2013 – February 2014) and 2014/2015 (November 2014 – February 2015). 5-days air-mass back-trajectories arriving at 00:00, 06:00, 12:00 and 18:00 GMT at Granada at 500 m a.g.l., were calculated and clustered using the Hysplit4 model (Draxler et al., 2013) for the aforementioned periods. Cluster analysis of air masses reaching Granada (Figure S2) point to significant differences between the three studied winter periods in terms of predominant air masses. During the winters 2012/2013 and

2014/2015 around 30% of the air masses were of regional/local origin (air masses traveling at low levels and at short distances from Granada) which might lead to lower dispersion of pollutants and higher EBC concentrations in these two periods compared to winter 2013/2014. However, in winter 2013/2014 there was an absence of air masses of regional/local origin and predominance of air masses originating from Canada and North Atlantic Ocean (around 70% of the air masses that affected Granada in this season). These air masses travelled long distances and at high altitudes, overpassing the Atlantic Ocean, and were likely featuring lower concentrations of pollutants. In fact, these air masses are usually associated with the lowest EBC concentration in the study area (Lyamani et al., 2011). Thus, the results indicate that the change in the synoptic conditions might explain the decrease in the EBC concentrations in winter 2013/2014 relative to the previous and following winters.

Figure 2: Monthly averages of equivalent black carbon, EBC, mass concentration and Absorption Ångström Exponent, AAE, at 370-520 nm measured at UGR. The whisker represents the standard deviation, the box limits the 25 and 75th percentiles and the central square and line are the mean and median values, respectively.

3.2. Biomass burning tracers

The AAE values as well as EBC concentrations showed a large seasonal variability, indicating a significant change in emission sources. In order to investigate the sources of these UV-absorbing particles, 24-h PM_{10} samples collected at UGR from September 2012 to September 2013 were analysed for biomass burning tracers such as levoglucosan, OC,

EC and K (Table 2). The information shown in Table 2 is split between the period November – February, when the impact of biomass burning emissions is expected to be higher, and the rest of the year. Note that K refers to total potassium in PM_{10} and not to its soluble fraction alone.

Figure 3 shows daily concentrations of levoglucosan together with daily average values of the levoglucosan/OC ratio and AAE. As can be seen, high AAE values were associated with an increase in levoglucosan mass concentrations during winter time (shaded area). Very low concentrations of levoglucosan were measured during the rest of the year (Table 2). During the study period, levoglucosan concentration varied significantly, from a minimum of 0.03 µg/m^3 up to the maximum of 0.57 µg/m^3. A winter average value of 0.25 µg/m^3 was calculated, showing an increased impact of biomass burning emissions during this season. The seasonality observed in levoglucosan mass concentrations is consistent with results from other European sites (Jedynska et al., 2015) and associated with higher emissions from biomass burning and poorer atmospheric dispersion. According with previous investigations (see Table 3), levoglucosan concentrations measured in Granada are in the lower range of values reported for other urban areas like Aveiro (Puxbaum et al., 2007), Graz (Caseiro et al., 2009) or Florence (Giannoni et al., 2012); but higher than the observed concentrations in The Netherlands (Jedynska et al., 2015), Vienna and Salzburg (Caseiro et al., 2009), London (Fuller et al., 2014) or Barcelona (Reche et al., 2012), among others. Winter OC and EC mass concentrations in Granada (Table 2) were significantly higher compared with the values listed in Table 3, leading to lower levoglucosan/OC ratios.

Table 2: Average mass concentration of some measured aerosol species and their ratios for winter (Nov-Feb) and the rest of the year. AAE: Absorption Ångström exponent in the wavelength range 370-520 nm.

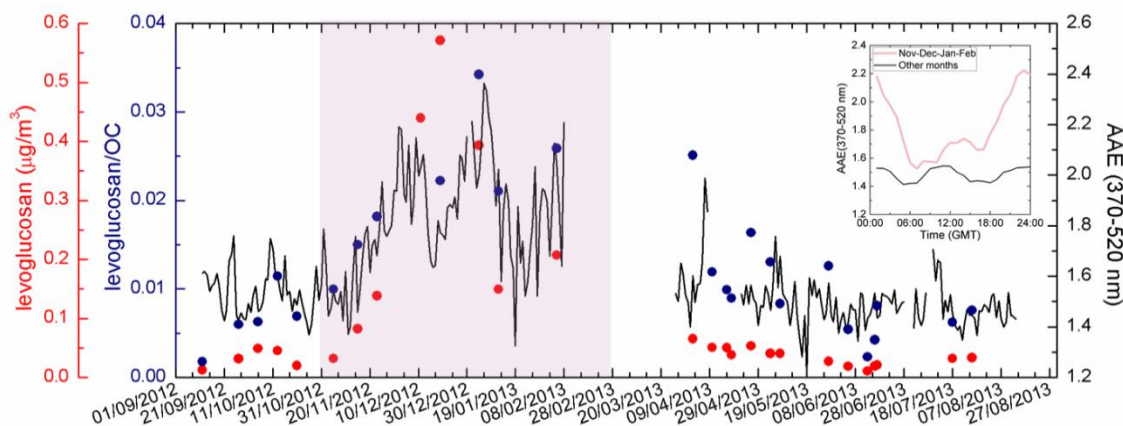|	PM_{10}	OC	EC	levoglucosan	OC/EC	levoglucosan/OC	K/levoglucosan	AAE
	(µg/m^3)				(dimensionless)			
Nov-Feb	34.2	9.0	2.7	0.25	3.1	0.02	2.1	1.8
Rest	29.8	4.4	1.8	0.04	2.7	0.01	8.4	1.5

Figure 3: Daily average values of AAE(370-520 nm), levoglucosan mass concentration and the ratio levoglucosan/OC measured at UGR for 1-year period from September 2012 to August 2013. The sub-plot shows the diurnal evolution of AAE(370-520 nm) for the shaded period (pink) and the rest of the year (black). Error bars have been omitted for better visualization.

Table 3: Mass concentrations of levoglucosan, Organic and Elemental Carbon reported for different environments. The measurement site, period and size cut are also reported. The table is sorted according with the publication year. *bonfire event

Site	Period	Size cut	Levoglucosan ($\mu g/m^3$)	OC	EC	Reference
Aveiro (Portugal)	Winter	PM$_{2.5}$	1.290	--	--	Puxbaum et al. (2007)
Vienna (Austria)	Winter	PM$_{10}$	0.220	--	--	Caseiro et al. (2009)
Graz (Austria)			0.683	--	--	
Salzburg (Austria)			0.293	--	--	
Barcelona (Spain)	Feb-March	PM$_{2.5}$	0.060	3.6	1.5	Reche et al. (2012)
Florence (Italy) (urban background)	Winter	PM$_{2.5}$	0.371	--	--	Giannoni et al. (2012)
Florence (Italy) (urban traffic)	Winter	PM$_{2.5}$	0.355	--	--	
London (United Kingdom)	Winter	PM$_{10}$	0.160	--	--	Fuller et al. (2014)
Riccione (Italy)	March-April*	PM$_{2.5}$	0.200	3.0	0.3	Vassura et al. (2014)
Oslo (Norway)	Winter	PM$_{2.5}$	0.294	2.13	--	Jedynska et al. (2015)
Netherlands			0.120	1.96	--	
Munich/Augsburg (Germany)			0.144	1.56	--	
Catalonia (Spain)			0.152	3.50	--	
Bologna (Italy)	February	PM$_{2.5}$	0.301	4.7	1.3	Pietrogrande et al. (2015)
San Pietro (Italy)	February		0.342	4.6	0.8	
Košetice (Hungary)	Winter	PM$_{2.5}$	0.237	6.0	0.8	Schwarz et al. (2016)

EBC mass concentration determined with the Aethalometer and averaged over the measuring time (24 hours) of the filter samples correlate well with EC mass concentration, with $R^2 = 0.98$ (Figure S3 in the Supplementary material). Only one sample, corresponding to 19 December 2012, falls out of the general trend, showing high EBC concentrations compared with EC (EBC and EC concentrations of 8.0 μg/m^3 and 3.9 μg/m^3, respectively). This day was characterized by high OC and levoglucosan concentrations (highest of the time-series with OC mass concentration of 25.7 μg/m^3 and levoglucosan of 0.57 μg/m^3). The high EBC concentration determined with the Aethalometer during 19 December could be due to this biomass burning event associated with absorption by organic compounds at 880 nm and/or to bias in Aethalometer measurements at high organic aerosol concentration (Lack et al., 2008). However, a systematic bias in the EBC-EC relationship as a function of the OC/EC ratio was not observed (color scale in Figure S3).

A relatively good correlation was found between AAE and levoglucosan mass concentration ($R^2 = 0.43$) and no correlation was found between AAE and the ratios OC/EC and K/levoglucosan. The lack of correlation with the ratio K/levoglucosan can be explained on the basis that K from biomass burning is mainly emitted in the fine fraction and K in PM$_{10}$ is not an appropriate biomass burning tracer. Coarse K may have other sources than biomass burning (for example crustal and marine origin) (Reche et al., 2012; Nava et al., 2015). The ratio levoglucosan/OC has been widely used in the literature to identify episodes of biomass burning (e.g., Reche et al., 2012; Zhang et al., 2014). The good correlation obtained between AAE and the levoglucosan/OC ratio ($R^2 = 0.61$) suggests that AAE can be used as well as biomass burning tracer; with the advantage of providing highly-time resolved data.

Sub-plot in Figure 3 shows the average diurnal evolution of AAE for the period November-February (pink line) when the levoglucosan concentrations were highest compared to the rest of the year (black line). AAE was higher during this period, as shown before, but especially during the evening-night hours. This diurnal pattern may be related with the average wind pattern affecting the area; easterly winds predominate during daytime and westerly winds predominate at night-time. Thus, pollutants emitted in the rural area nearby Granada during the day (agricultural waste burning) and in the late afternoon and evening (domestic heating based on biomass burning) can be transported towards the city during the night. Another hypothesis explaining the AAE diurnal pattern

is that the strong signal of the black carbon emitted by road traffic activity (fossil fuel combustion) dominates and can partially mask the influence of biomass burning emissions in the AAE during the day hours. During the evening-night hours, when the emissions from road traffic are reduced, the effect of biomass burning emissions in the AAE is more noticeable.

3.3. Identification of biomass burning sources

For identifying UV-absorbing aerosol sources we used the conditional bivariate probability function, CBPF, method. This method indicates the potential of a source region to contribute to high levels of the analyzed variable (Uria-Tellaetxe and Carslaw, 2014). The ordinary CPF (Conditional Probability Function, Ashbaugh et al., 1985) method estimates the probability that the measured concentration exceeds a set threshold criterion for a given wind sector. CBPF (Uria-Tellaetxe and Carslaw, 2014) couples CPF with wind speed as a third variable. This kind of analysis, CPF and CBPF, have been typically used with pollutant concentrations to identify pollution sources (e.g., Uria-Tellaetxe and Carslaw, 2014; Stojic et al., 2015; Khan et al., 2016). It can be also applied to other variables such as intensive aerosol optical properties (Titos et al., 2014b) allocating the observed variable to cells defined by ranges of wind direction and wind speed. We have applied this technique to hourly AAE(370-520 nm) values in combination with wind speed and direction data aiming to identify potential sources of UV-absorbing aerosols related with biomass burning emissions. CBPF is defined as:

$$CBPF_{\Delta\theta,\Delta u} = \frac{m_{\Delta\theta,\Delta u}|_{AAE\geq 2.4}}{n_{\Delta\theta,\Delta u}} \qquad (Eq.\ 5)$$

Where $m_{\Delta\theta,\Delta U}$ is the number of data-points (1 hour averages) in the wind sector $\Delta\theta$ with wind speed in the interval Δu having AAE values greater than a threshold value. In this case, the threshold value was calculated as the 90th percentile corresponding with AAE = 2.4. The total number of samples in that wind direction-speed interval is noted as $n_{\Delta\theta,\Delta u}$.

Figure 4 shows the CBPF for AAE in the period November 2012-February 2013 calculated for AAE higher than the 90th percentile (2.4). AAE is used here due to the high temporal resolution of this variable and its capability to identify biomass burning episodes as shown before. The CBPF analysis points towards a biomass burning source during winter located west and relatively close to the measurement site, UGR. As shown in Figure 1 this direction corresponds with agricultural farms and rural areas nearby Granada

where burnt of agricultural waste and use of biomass burning as heating source is frequent. However, the high complexity of the meteorological and orographic situation coupled with various emission sources make very difficult to discriminate between burning of agricultural waste and residential biomass burning.
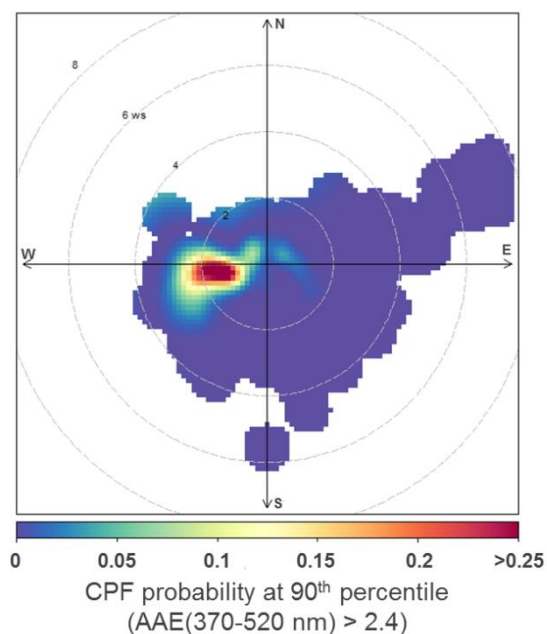

Figure 4: CBPF plot for AAE higher than the 90th percentile as a function of wind speed (m/s) and direction for the measurements obtained at UGR during the period November 2012 - February 2013.

3.4. Quantification of carbonaceous aerosols from biomass burning sources

3.4.1 Mono-tracer approach

A number of chemical compounds can be linked to biomass combustion emissions. For example, ambient concentrations of some anhydrosugars, and many other substances have been used as indicators of emissions from biomass burning. When the emission ratios of one of these tracers in PM and/or in CM are known, the contribution of wood burning at a receptor site can be calculated based on the concentration of the considered tracer at this site. Levoglucosan is a commonly used mono-tracer for biomass burning, as it is almost exclusively formed during cellulose pyrolysis.

The biomass burning OC, OC_{bb}, can be calculated with the mono-tracer approach assuming an emission ratio of levoglucosan and OC (Puxbaum et al., 2007; Jedynska et al., 2015). As suggested by Caseiro et al. (2009), an accurate estimation using this approach require using site-specific emission factors that consider both the wood species

actually burnt and the type of appliances in use. As this information was unknown for our study, we utilized results in emission factors from published field studies. Fine et al. (2004) reported an OC/levoglucosan emission ratio of 7.35 from test combustion in fireplaces and stoves; while, according with (Andreae and Merlet, 2001; Puxbaum et al., 2007) higher ratios are expected for open fires. In the study of Gelencsér et al. (2007), emission ratios in the range [6, 12.5] were used.

Using the range of values proposed by Gelencsér et al. (2007), a mass concentration of OC_{bb} in the range [1.3, 3.2] $\mu g/m^3$ was obtained for the period November-February in Granada. For this period, biomass burning contributed between 17 to 35% to the total organic carbon depending on the emission factor used. For the rest of the year the contribution of biomass smoke to OC was lower than 10%. Pietrogrande et al. (2015) estimated a biomass burning contribution of about 33% to OC in northern Italy during winter using an emissions factor of 6.6. Jedynska et al. (2015) estimated the contribution of wood smoke to OC in $PM_{2.5}$ using an emission factor of 5.6 and obtained a contribution of 24% (Catalonia), 34% (Netherlands), 51% (Munich/Ausburg) and 77% (Oslo) during winter. Significantly lower contributions were reported for the warm period (5%, 12%, 14% and 8% for Catalonia, Netherlands, Munich/Ausburg and Oslo, respectively).

3.4.2 Aethalometer model

Sandradewi et al. (2008) introduced the Aethalometer model to infer the contribution of road traffic and wood burning emissions to carbonaceous matter using a seven-wavelength Aethalometer in the Swiss Alpine Valley. The method itself assumes that the spectral aerosol absorption is composition-dependent, and that only road traffic and wood burning are contributing to this attenuation. It is well known that other aerosol species like mineral dust (Fialho et al., 2014; Valenzuela et al., 2015) or products from coal combustion (Bond et al., 2002) may contribute to the absorption in the UV range. Despite of this, the Aethalometer model has been widely used during the past years to apportion the contribution of fossil fuels and biomass burning emission sources (e.g., Sandradewi et al., 2008; Harrison et al., 2012; Fuller et al., 2014; Ealo et al., 2016).

The equations that relate the absorption coefficients (σ_{ap}), the wavelengths, and the AAE for fossil fuel and biomass burning (AAE_{ff} and AAE_{bb}, respectively) are:

$$\frac{\sigma_{ap}(370\,nm)_{ff}}{\sigma_{ap}(950\,nm)_{ff}} = \left(\frac{370}{950}\right)^{-AAE_{ff}} \tag{Eq. 6}$$

$$\frac{\sigma_{ap}(370\ nm)_{bb}}{\sigma_{ap}(950\ nm)_{bb}} = \left(\frac{370}{950}\right)^{-AAE_{bb}} \qquad\qquad \text{(Eq. 7)}$$

$$\sigma_{ap}(370\ nm) = \sigma_{ap}(370\ nm)_{ff} + \sigma_{ap}(370\ nm)_{bb} \qquad\qquad \text{(Eq. 8)}$$

$$\sigma_{ap}(950\ nm) = \sigma_{ap}(950\ nm)_{ff} + \sigma_{ap}(950\ nm)_{bb} \qquad\qquad \text{(Eq. 9)}$$

For given AAE_{ff} and AAE_{bb} values and using the experimental data of the light absorption measurements, $\sigma_{ap}(370\ nm)$ and $\sigma_{ap}(950\ nm)$, the values for $\sigma_{ap}(370\ nm)_{ff}$, $\sigma_{ap}(370\ nm)_{bb}$, $\sigma_{ap}(950\ nm)_{ff}$ and $\sigma_{ap}(950\ nm)_{bb}$ can be computed with equations 6-9.

The source apportionment of carbonaceous material, CM, into the contribution of biomass burning, CM_{bb}, and fossil fuel combustion, CM_{ff}, can be estimated by applying a multiple linear regression, MLR (Eq. 10). In the MLR model, the constants C_2 and C_1 are inverse mass absorption cross section for biomass burning (at 370 nm) and fossil fuel (at 950 nm), respectively, and C_3 accounts for the constant contribution of organic aerosols (or can be considered as the model residual). CM_{bb} and CM_{ff} can be then calculated using Eq. 11-12 and constants C_2 and C_1 from the MLR output.

$$CM = C_3 + C_2 \cdot \sigma_{ap}(370\ nm)_{bb} + C_1 \cdot \sigma_{ap}(950\ nm)_{ff} \qquad\qquad \text{(Eq. 10)}$$

$$CM_{bb} = C_2 \cdot \sigma_{ap}(370\ nm)_{bb} \qquad\qquad \text{(Eq. 11)}$$

$$CM_{ff} = C_1 \cdot \sigma_{ap}(950\ nm)_{ff} \qquad\qquad \text{(Eq. 12)}$$

One of the main weaknesses of this model relies in the assumption of AAE_{ff} and AAE_{bb}. The stability of the model output with respect to AAE_{ff} and AAE_{bb} has been determined by looking at the variations in C_1, C_2 and C_3 for varying AAE_{ff} and AAE_{bb} in the range [0.8, 1.2] and [1.8, 2.2], respectively (Figure 5). In all cases, the goodness of the MLR fit was good with $R^2 > 0.9$. The results shown in Figure 5 indicate that the contribution of other organic aerosols to CM (which can also be interpreted as the residual of the model) was small ($C_3 < 0.1$ µg/m^3) and independent of AAE_{ff} and AAE_{bb}. These two features (small C_3 and independency of AAE_{ff} and AAE_{bb}) are indicative that the model performs well and that there are no large unknown sources. C_2 was independent of AAE_{ff} and showed low variability with respect to AAE_{bb}. On the contrary, C_1 was dependent on AAE_{ff} showing higher variation with values in the range [0.2, 0.5] $\times 10^6$ µg/m^2. These C_i values and their dependence with AAE_{ff} and AAE_{bb} are in agreement with previous

studies (e.g. Sandradewi et al., 2008; Favez et al., 2010). The results obtained suggest that the model can be considered stable, especially with respect to AAE_{bb}.
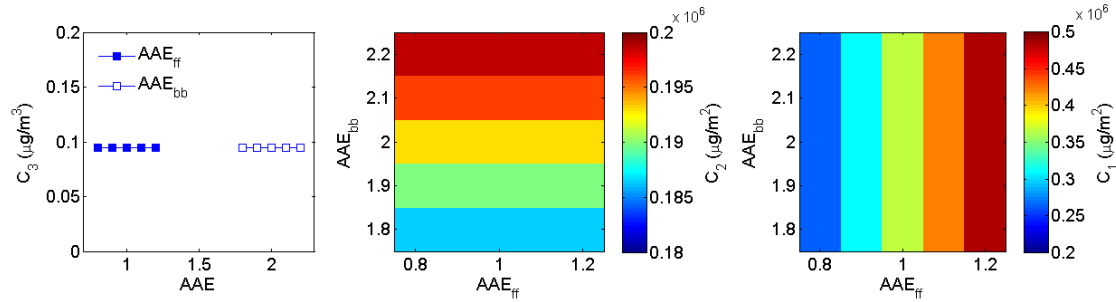

Figure 5: Dependence of model constants (C_3, C_2 and C_1) with AAE_{ff} and AAE_{bb}.

The performance of the Aethalometer model to estimate source contributions for varying AAE_{ff} and AAE_{bb} values has been evaluated based on the correlation between measured levoglucosan mass concentrations and BC_{bb} concentrations from the Aethalometer model. As the first step, we have used BC_{bb} instead of CM_{bb} in this evaluation exercise because both levoglucosan and BC_{bb} are of primary origin while CM_{bb} can be from primary and secondary origin. Figure 6a displays the R^2 of the fitting levoglucosan-BC_{bb} as a function of AAE_{ff}. A strong correlation was found between levoglucosan and BC_{bb} concentrations. R^2 above 0.9 was obtained for AAE_{ff} in the range [0.9, 1.1], while the variation of R^2 with AAE_{bb} was negligible (not shown). The results from both methods (levoglucosan tracer and Aethalometer model) were correlated but the levoglucosan-BC_{bb} regression slope cannot be used to evaluate the model for variations in AAE_{ff} and AAE_{bb}. Nevertheless, zero concentrations of both tracers are expected to occur at the same time. The regression intercept of levoglucosan on BC_{bb} should be zero if the methods are consistent and both tracers experience the same rate of atmospheric removal (Fuller et al., 2014). Figure 6b shows the intercept of the fit for different AAE_{ff} and AAE_{bb} combinations. The intercept was closest to zero for $AAE_{ff} = 1.1$. For this AAE_{ff} value, the variation in the magnitude of the intercept was almost independent of AAE_{bb}. Thus, based on the goodness of the fit and the zero-intercept, $AAE_{ff} = 1.1$ seems to be the optimal value for our study. The magnitude of the retrieved concentrations of BC_{bb} (Figure 6c) varied with the AAE_{bb} and AAE_{ff} (same occurs for CM_{bb}, not shown). For example, for fixed $AAE_{ff} = 1.1$, BC_{bb} varied from 0.16 µg/m^3 ($AAE_{bb} = 2.2$) to 0.27 µg/m^3 ($AAE_{bb} = 1.8$) and for fixed $AAE_{bb} = 2$, BC_{bb} varied from 0.45 µg/m^3 ($AAE_{ff} = 0.8$) to 0.07 µg/m^3 ($AAE_{ff} = 1.2$).
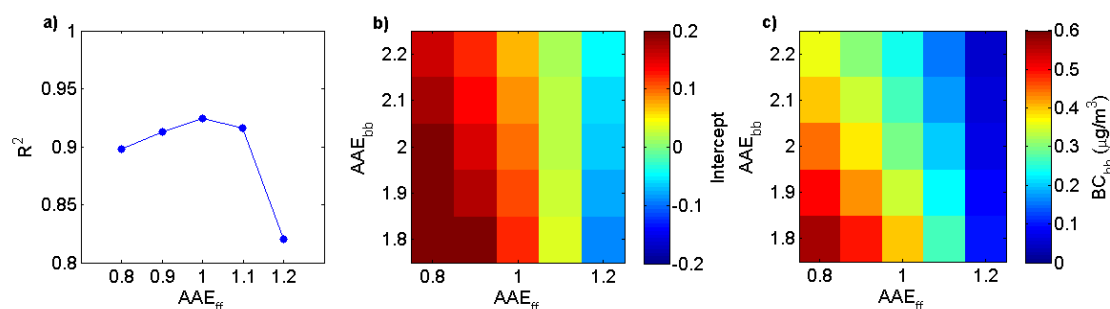
Figure 6: R^2 of the fitting levoglucosan-BC_{bb} for UGR station during the period September 2012 – August 2013 as a function of the AAE_{ff} used (a), intercept of the fitting (b) and BC_{bb} mass concentrations (c) as a function of AAE_{bb} and AAE_{ff}.

Harrison et al. (2013) determined the most plausible AAE_{bb} by comparing the diurnal evolution of PM_{ff} and PM_{bb} (particulate matter from fossil fuel or biomass burning origin, respectively) for different AAE_{bb} values and looking for the most feasible behavior. Figure 7 shows CM_{ff} and CM_{bb} diurnal evolution obtained with the Aethalometer model, using an $AAE_{ff} = 1.1$ and for AAE_{bb} in the range [1.8-2.2], separated for the period November-February (upper panel) and the rest of the year (lower panel). CM_{ff} showed the expected behavior for this variable with two maxima in coincidence with traffic rush hours, and with higher concentrations in winter. In November-February, CM_{bb} showed higher values during the evening-night hours. During the rest of the year, CM_{bb} was substantially lower and it depicted a smooth two-peak diurnal pattern typical of traffic emissions. This may be due to failure of the model when the contribution of biomass burning is very low, being part of the CM erroneously attributed to biomass burning even though it corresponded to traffic emissions. Since biomass burning emissions are not expected during summer (domestic heating is not used and agricultural waste burning is not allowed), this is the most plausible explanation. This artifact occurred independently of the AAE_{bb} used. During winter, the diurnal evolutions of CM_{bb} and CM_{ff} retrieved for $AAE_{bb} = [1.8, 2.2]$ were very similar and provided realistic patterns for both biomass and fossil fuel contributions. In the light of the results, the most suitable values for the Aethalometer model are $AAE_{ff} = 1.1$ and $AAE_{bb} = 2$. The latter one has been selected as the central value in the range of values studied since all AAE_{bb} provided reasonable results and the various sensitivity tests carried out were not able to provide a more robust answer. Using these AAE values, the average CM_{bb} concentration in summer was 0.9 $\mu g/m^3$ (12% of the total CM), which can be used as the absolute uncertainty of the source apportionment model.
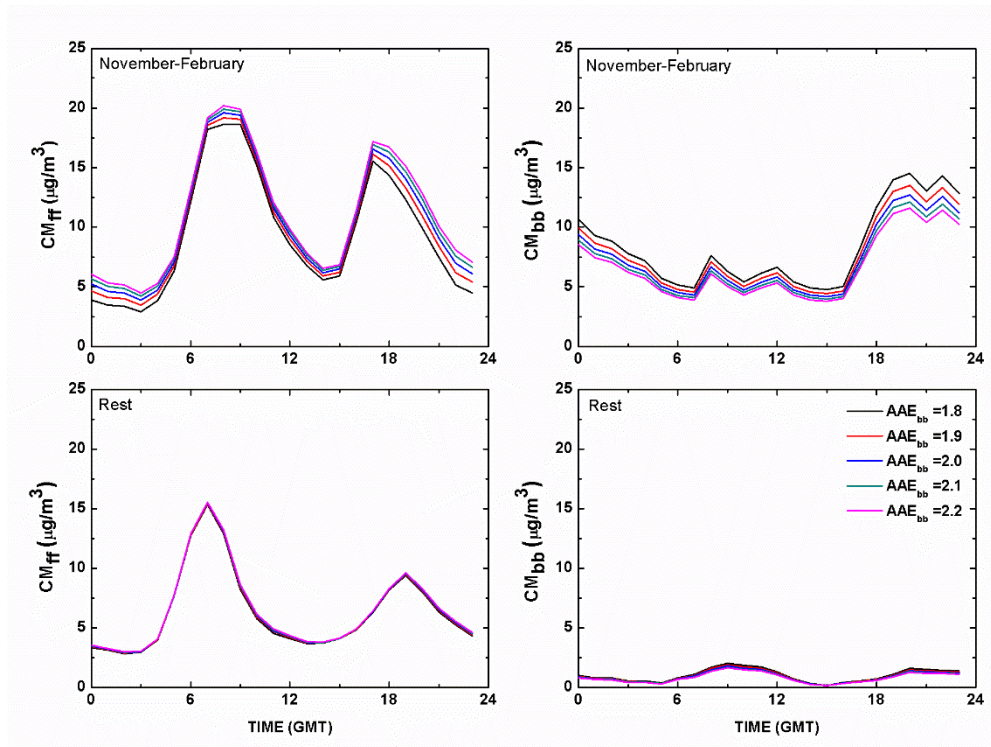
Figure 7: Diurnal evolution of CM$_{ff}$ and CM$_{bb}$ retrieved for UGR during the period November 2012 – February 2013 (upper panel) and the rest of the year under study (lower panel) for AAE$_{ff}$ = 1.1 and different combinations of AAE$_{bb}$ in the Aethalometer model.

3.5. Spatial variability

During 1-year period starting on June 2014, continuous measurements of aerosol absorption at multiple wavelengths were performed at three experimental sites within the city of Granada, Spain (Figure 1), to explore their spatial variability. Table 4 shows the mean CM$_{bb}$ and CM$_{ff}$ concentrations calculated at the three experimental sites. The Aethalometer model has been applied using AAE$_{ff}$ = 1.1 and AAE$_{bb}$ = 2.0, which has been proven to be the optimal values for our site. Consequently, to estimate the CM$_{bb}$ and CM$_{ff}$ mass concentrations we have used as constants values C$_2$ = 0.193 g/m^2 and C$_1$ = 0.422 g/m^2, with the contribution from other sources C$_3$ = 0.1 μg/m^3, all according to results previously shown in Figure 5. Doing this, we assumed that these constants were the same in the three sites and that they remained constant over time.

The model output shows that Granada urban area is highly influenced by biomass burning emissions during winter. Similar contributions to CM from both fossil fuel combustion and biomass burning sources were determined at UGR (47%) and PC (41%), while lower contribution of biomass burning to CM were obtained in the city center (30% in GV). In

terms of absolute concentrations, UGR is the station with higher influence of biomass burning emissions ($CM_{bb} = 7.6 \pm 1$ µg/m^3) likely due to its proximity to the rural area and agricultural land. On the other hand, GV is the station with higher influence of fossil fuel emissions, with average CM_{ff} of 13.1 ± 1 µg/m^3. Slightly lower concentrations of both CM_{bb} and CM_{ff} were found at PC compared to UGR, but of similar magnitude considering the estimated uncertainties. Outside of the period November-February, CM concentrations were dominated by fossil fuel emissions at all sites with negligible contribution of biomass burning.

Table 4: Mean CM$_{bb}$ and CM$_{ff}$ in µg/m^3 and contribution of CM$_{bb}$ retrieved for UGR, PC and GV stations during the period November 2014 – February 2015 using the Aethalometer model (AAE$_{ff}$ = 1.1 and AAE$_{bb}$ = 2.0; C$_3$ = 0.1 µg/m^3, C$_2$ = 0.193 g/m^2 and C$_1$ = 0.422 g/m^2). The absolute uncertainty in CM is estimated in 1 µg/m^3.

	November 2014 – February 2015		
	CM$_{ff}$	CM$_{bb}$	% CM$_{bb}$
	µg/m^3		
UGR	8.5	7.6	(47 ± 6) %
PC	8.1	5.8	(41 ± 7) %
GV	13.1	5.7	(30 ± 5) %

3.6. Effectiveness of implemented pollution abatement measures

A large number of air quality plans have been implemented in the past years in urban areas with the aim of reducing air pollution (Harrison et al., 2015), most of them focusing on traffic emissions (Invernizzi et al., 2011; Titos et al., 2015). In Granada, the public transportation was re-organized in June 2014 to reduce overlap between lines in the city centre. In addition, a new bus line operated by new buses with lower emissions passing through Gran Vía street, GV, was implemented. Titos et al. (2015) showed that EBC concentrations were reduced in 37% in GV in the two weeks just after the new system was operational. No changes were observed in other parts of the city like PC or UGR (Titos et al., 2015). With the objective of re-evaluating the effectiveness of this measure in the medium-term we have selected two weeks before the measure implementation in 2014 and the same two weeks one year after, in 2015. The two periods were meteorologically comparable so differences in EBC are likely due only to changes in emissions rather than in meteorological conditions. The results showed a decrease of 20% in EBC mass concentrations at GV and no significant changes in UGR and PC stations. This decrease is still significant even though it is almost half of the decrease observed just

after the new system was implemented (Titos et al., 2015). Without any information on the number of buses, motorbikes and cars passing this street it is difficult to determine whether this difference is due to an increase in the emissions in 2015. The observed increase can be partially attributed to age of the bus fleet operating in the new line in one year of the implementation or the driving regime, both of which may have been more advantageous to air quality in the early stages of the implementation. Although meteorology plays an important role on the measured EBC concentrations, the fact that EBC concentrations did not vary significantly in UGR and PC for the same period suggests that the changes observed in GV can be attributed to changes in emissions.

Recently, the public transport in Gran Via has been reorganized once again due to complaints from the citizens, and two more bus lines transit again this street. Thus, EBC concentrations are expected to increase in the following years in this area and probably reach the EBC levels of 2014 prior to the implementation of the new bus transportation system.

4. Conclusions

The temporal and spatial variability of carbonaceous aerosols have been investigated in this study. A clear seasonal cycle with higher EBC mass concentrations and AAE during winter was observed during the 3-years period analysed at UGR. High AAE values point to an increase in UV-absorbing aerosols during winter time likely related with biomass burning emissions (dust intrusions are not frequent during this time of the year in the study area). The increase concentration at UGR of biomass burning tracers such as levoglucosan during winter confirm that biomass burning is an additional source of absorbing aerosols during the cold season. The good correlation between AAE and levoglucosan and levoglucosan/OC ratio suggests that AAE can be used as a parameter to identify biomass burning aerosols. The Aethalometer model has been used to provide a quantitative estimation of the contribution of biomass burning to the total carbonaceous matter. Optimal AAE for fossil fuel and biomass burning were estimated to be 1.1 and 2, respectively. A set of sensitivity tests have been performed in order to optimize the Aethalometer model and provide realistic results. The results were then applied to multiple sites within the city of Granada. The influence of biomass burning emissions was lower in the city centre (GV site), while it has a profound impact on CM concentrations during winter in UGR and PC.

The biomass burning source was identified west from the city, in the rural area nearby Granada. However, it is not clear whether this source correspond with open biomass burning of agricultural waste or biomass burning from domestic heating or both. Both practices are common in the rural area surrounding Granada during the cold season, and especially domestic heating based on olive pits burning has significantly increased over the past years. Further measurements in this rural area are needed to address the origin of biomass burning and its impact in the air quality of the urban area. On-line real-time chemical composition might also help to improve our understanding on biomass burning and fossil fuel contribution to carbonaceous matter.

Implemented abatement measures focusing on traffic restrictions and on optimizing public transportation in the city center led to significant decrease of EBC mass concentrations but the extent of these measures was reduced to the area where the restrictions were implemented. Thus, to improve urban air quality, traffic regulations should be implemented in wider areas and not only on specific and limited areas of the city centre. Furthermore, future pollution management strategies should take into account that biomass burning can be an important aerosol source during winter season. In fact, biomass burning contributed to CM in a similar extent than fossil fuel combustion. Pollution problems in Granada, and probably in most urban areas, should be seen from a wider perspective and targeted accordingly.

References

ACTRIS Intercomparison Workshop for Integrating Nephelometer and Absorption Photometers, 2013, http://www.wmo-gaw-wcc-aerosol-physics.org/files/ACTRIS-intercomparison-workshop-integrating-nephelometer-and-absorption-photometer-02-03-2013.pdf, (last accessed September 2016)

Alados-Arboledas, L., Müller D., Guerrero-Rascado J.L., Navas-Guzmán F., Pérez-Ramírez D., Olmo F.J.: Optical and microphysical properties of fresh biomass burning aerosol retrieved by Raman lidar, and star- and sun-photometry, Geophys. Res. Lett., 38, L01807, 2011.

Alfarra, M.R., Prévôt, A.S., Szidat, S., Sandradewi, J., Weimer, S., Lanz, V.A., Schreiber, D., Mohr, M., Baltensperger, U.: Identification of the mass spectral signature of organic aerosols from wood burning emissions. Environmental Science & Technology 41 (16), 5770-5777, 2007.

Alves, C., Vicente, A., Nunes, T., Gonçalves, C., Fernández, A.P., Mirante, F., Tráelo, L., Sánchez de la Campa, A.M., Querol, X., Caseiro, A., Monteiro, C., Eytyungina, M., Pio, C.: Summer 2009 wildfires in Portugal: emission of trace gases and aerosol composition. Atmos. Environ., 45, 641-649, 2011.

Andreae M.O., Merlet P.: Emission of trace gases and aerosols from biomass burning, Global Biogeochem Cycles 15(4):955-966, 2001.

Ashbaugh L.L., Malm W.C., Sadeh W.Z.: A residence time probability analysis of sulfur concentrations at Grand Canyon National Park. Atmos. Environ., 19 (8), 1263-1270, 1985.

Beelen R, Hoek G, van den Brandt P, Goldbohm A, Fischer P, Schouten LJ, et al.: Long-term effects of traffic-related air pollution on mortality in a Dutch cohort (NLCS-AIR study). Environ. Health Perspect. 116:196–202, 2008.

Bergstrom, R. W., Russell, P. B., Hignett P.: Wavelength dependence of the absorption of black carbon particles: Predictions and results from the TARFOX experiment and implications for the aerosol single scattering albedo, J. Atmos. Sci., 59, 567 – 577, 2002.

Bond T. C., Covert D. S., Kramlich J.C., Larson T. V., Charlson R. J.: Primary particle emissions from residential coal burning: Optical properties and size distributions, J. Geophys. Res., 107(D21), 8347, doi:10.1029/2001JD000571, 2002.

Brauer M, Hoek G, van Vliet P, Meliefste K, Fischer PH, Wijga A, et al.: Air pollution from traffic and the development of respiratory infections and asthmatic and allergic symptoms in children. Am J Respir Crit Care Med 166:1092–1098, 2002.

Bravo-Aranda J. A., Titos G., Granados-Muñoz M. J., Guerrero-Rascado J. L., Navas-Guzmán F., Valenzuela A., et al.: Study of mineral dust entrainment in the planetary boundary layer by lidar depolarisation technique, Tellus B, 67, 26180, 2015.

Caseiro A., Bauer H., Schmidl C., Pío C.A., Puxbaum H.: Wood burning impact on PM10 in three Austrian regions, Atmos. Environ., 43, 2186-2195, 2009.

Cavalli F., Viana M., Yttri K.E., Genberg J., Putaud J.P.: Toward a standardised thermal-optical protocol for measuring atmospheric organic and elemental carbon: the EUSAAR protocol. Atmos. Meas. Tech., 3-1, 78-89, 2010.

Cazorla A., Bahadur R., Suski K. J., Cahill J. F., Chand D., Schmid B., et al.: Relating aerosol absorption due to soot, organic carbon, and dust to emission sources determined from in-situ chemical measurements, Atmos. Chem. Phys., 13, 9337-9350, 2013.

Dambruoso P., de Gennaro G., Di Gilio A., Palmisani J., Tutino M.: The impact of infield biomass burning on PM levels and its chemical composition, Environ. Sci. Pollut. Res., 21:13175-13185, 2014.

Draxler, R. R., Stunder B., Rolph G., Stein A., Taylor A.: HYSPLIT4 User's Guide, NOAA Air Resources Laboratory, 2013 (http://www.arl.noaa.gov/documents/reports/hysplit_user_guide.pdf, last access: February 2014).

Drinovec L., Močnik G., Zotter P., Prévôt A.S.H., Ruckstuhl C., Coz E., et al.: The "dual-spot" Aethalometer: an improved measurement of aerosol black carbon with real-time loading compensation. Atmos. Meas. Tech. Discuss., 7, 10179-10220, 2014.

Ealo M., Alastuey A., Ripoll A., Pérez N., Minguillón M. C., Querol X., Pandolfi M.: Detection of Saharan dust and biomass burning events using near real-time intensive aerosol optical properties in the northwestern Mediterranean, Atmos. Chem. Phys. , 16, 12567–12586, doi:10.5194/acp-16-12567-2016, 2016.

Fialho P., Cerqueira M., Pio C., Cardoso J., Nunes T., Custódio D., et al.: The application of a multi-wavelength Aethalometer to estimate iron dust and black carbón concentrations in the marine boundary layer of Cape Verde, Atmos. Environ., 97, 136-143, 2014.

Fine P. M., Cass G. R., Simoneit B. R. T.: Chemical characterization of fine particle emissions from the wood stove combustion of prevalent United States tree species, Environ. Eng. Sci., 21, 705–721, 2014.

Fuller G. W., Sciare J., Lutz M., Moukhtar S., Wagener S.: New directions: Time to tackle urban wood burning?, Atmos. Environ., 68, 295-296, 2013.

Fuller G. W., Tremper A. H., Baker T. D., Yttri K. E., Butterfield D.: Contribution of wood burning to PM10 in London, Atmos. Environ., 87, 87-94, 2014.

Gelencsér A., May B., Simpson D., Sánchez-Ochoa A., Kasper-Giebl A., Puxbaum H., et al.: Source apportionment of PM2.5 organic aerosol over Europe: Primary/secondary, natural/anthropogenic, and fossil/biogenic origin, J. Geophys. Res., 112, D23S04, 2007.

Giannoni M., Martellini T., Del Bubba M., Gambaro A., Zangrando R., Chiari M., et al.: The use of levoglucosan for tracing biomass burning in PM2.5 samples in Tuscany (Italy), Environ. Poll., 167, 7-15, 2012.

Granados-Muñoz M.J., Navas-Guzmán F., Bravo-Aranda J.A., Guerrero-Rascado J.L., Lyamani H., Fernández-Gálvez J., et al.: Automatic determination of the planetary

boundary layer height using lidar: One-year analysis over southeastern Spain, J. Geophys. Res., 117, D18208, doi:10.1029/2012JD017524, 2012.

Guerrero-Rascado J.L., Ruiz B., Alados-Arboledas L.: Multispectral Lidar characterization of the vertical structure of Saharan dust aerosol over southern Spain, Atmos. Environ., 42, 2668–2681, 2008.

Hamilton R.S., Mansfield T.A.: Airborne particulate elemental carbon: its sources, transport and contribution to dark smoke and soiling. Atmos. Environ., 25, 715–723, 1991.

Hansen A.D.A, Novakov R.: The Aethalometer - an instrument for the real-time measurement of optical absorption by aerosol particles. Sci. Total Environ., 36, 191-196, 1984.

Harrison R. M., Beddows D. C. S., Hu L., Yin J.: Comparison of methods for evaluation of wood smoke and estimation of UK ambient concentrations, Atmos. Chem. Phys., 12, 8271-8283, 2012.

Harrison R. M., Beddows D. C. S., Jones A. M., Calvo A., Alves C., Pio C.: An evaluation of some issues regarding the use of aethalometers to measure woodsmoke concentrations, Atmos. Environ., 80, 540-548, 2013.

Herich H., Gianini M.F.D., Piot C., Močnik G., Jaffrezo J.-L., Besombes J.-L., Prévôt A.S.H., Hueglin C.: Overview of the impact of wood burning emissions on carbonaceous aerosols and PM in large parts of the Alpine region, Atmos. Environ., 89, 64-75, 2014.

Hoek G, Brunekreef B, Verhoeff A, van Wijnen J, Fischer P.: Daily mortality and air pollution in The Netherlands. J Air Waste Manage Assoc 50:1380–1389, 2000.

Janssen NA, Gerlofs-Nijland ME, Lanki T, Salonen RO, Cassee F, Hoek G et al.: Health effects of black carbon. Copenhagen: WHO Regional Office for Europe, 2012 (http://www.euro.who.int/en/health-topics/environment-and-health/air-quality/publications/2012/health-effects-of-black-carbon, accessed September 2016).

Jedynska A., Hoek G., Wang M., Eeftens M., Cyrys J., Beelen R., et al.: Spatial variations of levoglucosan in four European study areas, Sci. Total Environ., 505, 1072-1081, 2015.

Khalil, M.A.K., Rasmussen, R.A.: Tracers of wood smoke. Atmos. Environ., 37, 1211-1222, 2003.

Khan M.B., Masiol M., Formenton G., Di Gilio A., de Gennaro G., Agostinelli C., Pavoni B.: Carbonaceous PM2.5 and secondary organic aerosol across the Veneto region (NE Italy), Sci. Total. Environ., 542, 172-181, 2016.

Kirchstetter, T. W., Novakov, T., Hobbs, P.V.: Evidence that the spectral dependence of light absorption by aerosols is affected by organic carbon, J. Geophys. Res., 109, doi: 10.1029/2004JD004999, 2004.

Kostenidou E., Kaltsonoudis C., Tsiflikiotou M., Louvaris E., Russel L. M., Pandis S. N.: Burning of olive tree branches: a major organic aerosol source in the Mediterranean, Atmos. Chem. Phys., 13, 8797-8811, 2013.

Lack D. A., Cappa C. D., Covert D. S., Baynard T., Massoli P., Sierau B., Bates T. S., Quinn P. K., Lovejoy E. R., Ravishankara A. R.: Bias in Filter Based Aerosol Light Absorption Measurements Due to Organic Aerosol Loading: Evidence from Ambient Measurements, Aerosol Sci. Tech., 42, 1033–1041, 2008.

Larssen, S., Laupsa, H., SlØrdal, H.S., TØnnesen Hagen, L.O.: Calculation of PM2.5 from Wood Burning in Oslo, Norwegian. Institute for Air Research (OR 28/2006), Kjeller (in Norwegian), 2006.

Lyamani H., Olmo F.J., Alados-Arboledas L.: Saharan dust outbreak over southeastern Spain as detected by sun photometer. Atmos. Environ. 39, 7276–7284, 2005.

Lyamani H., Olmo F.J., Alados-Arboledas L.: Light scattering and absorption properties of aerosol particles in the urban environment of Granada, Spain. Atmos. Environ., 42, 2630-2642, 2008.

Lyamani H., Olmo F.J., Alados-Arboledas L.: Physical and optical properties of aerosols over an urban location in Spain: seasonal and diurnal variability. Atmos. Chem. Phys., 10, 239-254, 2010.

Lyamani H., Olmo F.J., Foyo I., Alados-Arboledas L.: Black carbon aerosols over an urbana rea in south-eastern Spain: Changes detected after the 2008 economic crisis. Atmos. Environ., 45, 6423-6432, 2011.

Lyamani H., Fernández-Gálvez J., Pérez-Ramírez D., Valenzuela A., Antón M., Alados I., et al.: Aerosol properties over two urban sites in South Spain during an extended stagnation episode in winter season. Atmos. Environ., 62, 424-432, 2012.

Müller, T., Henzing J. S., de Leeuw G., Wiedensohler A., Alastuey A., Angelov H., et al.: Characterization and intercomparison of aerosol absorption photometers: result of two intercomparison workshops. Atmos. Measurement. Tech., 4, 245-268, 2011.

Nava S., Lucarelli F., Amato F., Becagli S., Calzolai G., Chiari M., et al.: Biomass burning contributions estimated by synergistic coupling of daily and hourly aerosol composition records, Sci. Total Environ., 511, 11-20, 2015.

Paatero, P.: Least square formulation of robust non-negative factor analysis, Chemometr. Intell. Lab. Syst., 3, 23–35, 1997.

Pakkanen T. A., Kerminen V. M., Ojanena C. H., Hillamo R. E., Aarnio P., Koskentalo T.: Atmospheric Black Carbon in Helsinki, Atmos. Environ., 34, 1497–1506, 2000.

Paraskevopoulou D., Liakakou E., Gerasopoulos E., Mihalopoulos N.: Sources of atmospheric aerosol from long-term measurements (5 years) of chemical composition in Athens, Greece, Sci. Total Environ., 527-528, 165-178, 2015.

Petzold, A., Schönlinner M.: Multi-angle Absorption photometry—a new method for the measurement of aerosol light absorption and atmospheric black carbon. J. Aerosol Sci., 35, 421–441, 2004.

Petzold A., Ogren J. A., Fiebig M., Laj P., Li S. M., Baltensperger U., et al.: Recommendations for reporting "black carbon" measurements, Atmos. Chem. Phys., 13, 8365-8379, 2013.

Piazzalunga A., Fermo P., Bernardoni V., Vecchi R., Valli B., De Gregorio M.A., A simplified method for levoglucosan quantification in wintertime atmospheric particulate matter by high performance anion-exchange chromatography coupled with pulsed amperometric detection, International Journal of Environmental Analytical Chemistry, 90:12, 934-947, 2010.

Pietrograde M.C., Bacco D., Ferrari S., Kaipainen J., Ricciardelli I., Riekkola M.L.,et al.: Characterization of atmospheric aerosols in the Po Valley during the supersito campaigns − Part 3: Contribution of Wood combustión to wintertime atmospheric aerosols in Emilia Romagna región (Northern Italy), Atmos. Environ., 122, 291-305, 2015.

Pope C.A., Dockery D.W.: Health effects of fine particulate air pollution: lines that connect. J Air Waste Manage Assoc; 56:709–42, 2006.

Puxbaum H., Caseiro A., Sánchez-Ochoa A., Kasper-Giebl A., Claeys M., Gelencsér A., et al.: Levoglucosan levels at background sites in Europe for assessing the impact of biomass combustion on the European aerosol background, J. Geophys. Res., 112, D23S05, 2007.

Querol X., Alastuey A., Rodríguez S., Plana F., Ruiz C.R., Cots N., et al.: PM10 and PM2.5 source apportionment in the Barcelona Metropolitan área, Catalonia, Spain, Atmos. Environ., 35, 6407-6419, 2001.

Querol, X., Alastuey, A., Viana, M., Moreno, T., Reche, C., Minguillon, M.C., et al., Variability of carbonaceous aerosols in remote, rural, urban and industrial environments in Spain: implications for air quality policy. Atmos. Chem. Phys., 13, 6185-6206, 2013.

Reche C., Viana M., Amato F., Alastuey A., Moreno T., Hillamo R., et al.: Biomass burning contributions to urban aerosols in a coastal Mediterranean City, Sci. Total Environ., 427-428, 175-190, 2012.

Sandradewi J., Prévôt A. S. H., Szidat S., Perron N., Alfarra M. R., Lanz V. A., et al.: Using Aerosol Light Absorption Measurements for the Quantitative Determination of Wood Burning and Traffic Emission Contributions to Particulate Matter, Environ. Sci. Technol., 42(9), 3316–3323, doi:10.1021/es702253m, 2008.

Sarigiannis D. A., Karakitsios S.P., Kermenidou M.: Health impact and monetary cost of exposure to particulate matter emitted from biomass burning in large cities, Sci. Total Environ., 524-525, 319-330, 2015.

Schuster G. L., Dubovik O., Holben, B. N.: Angstrom exponent and bimodal aerosol size distributions, J. Geophys. Res., 111(D7), D07207, doi:10.1029/2005JD006328, 2006.

Schwarz J., Cusack M., Karban J., Chalupníčková E., Havránek V., Smolík J., Zdímal V.: PM2.5 chemical composition at a rural background site in Central Europe,

including correlation and air mass trajectory analysis, Atmos. Res., 176-177, 108-120, 2016.

Segura S., Estellés V., Titos G., Lyamani H., Utrillas M. P., Zotter P., et al.: Determination and analysis of in situ spectral aerosol optical properties by a multiinstrumental approach, Atmos. Meas. Tech., 7, 2373-2387, doi:10.5194/amt-7-2373-2014, 2014.

Segura S., Estellés V., Esteve A. R., Marcos C. R., Utrillas M. P., Martínez-Lozano J. A.: Multiyear in-situ measurements of atmospheric aerosol absorption properties at an urban coastal site in western Mediterranean, Atmos. Environ., 129, 18-26, 2016.

Stojic A., Stanisic Stojic, S., Mijic Z., Sostaric A., Rajsic S.: Spatio-temporal distribution of VOC emissions in urban area based on receptor modeling, Atmos. Environ., 106, 71-79, 2015.

Titos G, Foyo-Moreno I, Lyamani H, Querol X, Alastuey A, Alados-Arboledas L.: Optical properties and chemical composition of aerosol particles at an urban location: An estimation of the aerosol mass scattering and absorption efficiencies, J. Geophys. Res., 117, D04206, doi:10.1029/2011JD016671, 2012.

Titos G., Lyamani H., Pandolfi M., Alastuey A., Alados-Arboledas L.: Identification of fine (PM1) and coarse (PM10-1) sources of particulate matter in an urban environment. Atmos. Environ., 89, 593-602, 2014a.

Titos G., Jefferson A., Sheridan P.J., Andrews E., Lyamani H., Alados-Arboledas L., Ogren J.A.: Aerosol light-scattering enhancement due to water uptake during TCAP campaign. Atmos. Chem. Phys. 14, 7031-7043, 2014b.

Titos G., Lyamani H., Drinovec L., Olmo F. J., Močnik G., Alados-Arboledas L.: Evaluation of the impact of transportation changes on air quality, Atmos. Environ., 114, 19-31, 2015.

Turpin B. J., Saxena P., Andrews E.: Measuring and simulating particulate organics in the atmosphere: Problems and prospects, Atmos. Environ., 34, 2983–3013, 2000.

Uria-Tellaetxe I., Carslaw D. C.: Conditional bivariate probability function for source indentification, Environmental Modelling & Software, 59, 1-9, 2014.

Valenzuela A., Olmo F. J., Lyamani H., Antón M., Quirantes A., Alados-Arboledas L.: Analysis of the columnar radiative properties retrieved during African desert dust events over Granada (2005–2010) using principal plane sky radiances and spheroids retrieval procedure, Atmos. Res., 104, 292–301, 2012.

Valenzuela A., Olmo F. J., Lyamani H., Antón M., Titos G., Cazorla A., Alados-Arboledas L.: Aerosol scattering and absorption Angström exponents as indicators of dust and dust-free days over Granada (Spain), Atmos. Res., 154, 1-13, 2015.

Vassura I., Venturini E., Marchetti S., Piazzalunga A., Bernardi E., Fermo P., Passarini F.: Markers and influence of open biomass burning on atmospheric particulate size and composition during a major bonfire event, Atmos. Environ., 82, 218-225, 2014.

Viana M., Reche C., Amato F., Alastuey A., Querol X., Moreno T., et al.: Evidence of biomass burning aerosols in the Barcelona urban environment during winter time, Atmos. Environ., 72, 81-88, 2013.

Vicente E. D., Duarte M. A., Tarelho L. A. C., Nunes T. F., Amato F., Querol X., et al.: Particulate and gaseous emissions from the combustion of different biofuels in a pellet stove, Atmos. Environ., 120, 15-27, 2015.

Weingartner E., Saathoff H., Schnaiter M., Streit N., Bitnar B., Baltensperger, U.: Absorption of light by soot particles: Determination of the absorption coefficient by means of aethalometers, J. Aerosol Sci., 34, 1445–1463, 2003.

Yttri K.E., Dye C., Slørdal L.H., Braathen O.A.: Quantification of monosaccharide anhydrides by liquid chromatography combined with mass spectrometry: application to aerosol samples from an urban and a suburban site influenced by small-scale wood burning. Journal of the Air & Waste Management 55, 1169-1177, 2005.

Zhang T., Cao J. J., Chow J. C., Shen Z.X., Ho K. F., Sai S., et al.: Characterization and seasonal variations of levoglucosan in fine particulate matter in Xi'an, China, Journal of the Air & Waste Management Association, 64:11, 1317-1327, 2014.

Zotter P., Herich H., Gysel M., El-Haddad I., Zhang Y., Močnik G., et al.: Evaluation of the absorption Ångström exponents for traffic and wood burning in the Aethalometer based source apportionment using radiocarbon measurements of ambient aerosol, Atmos. Chem. Phys. Discuss., doi:10.5194/acp-2016-621, 2016.
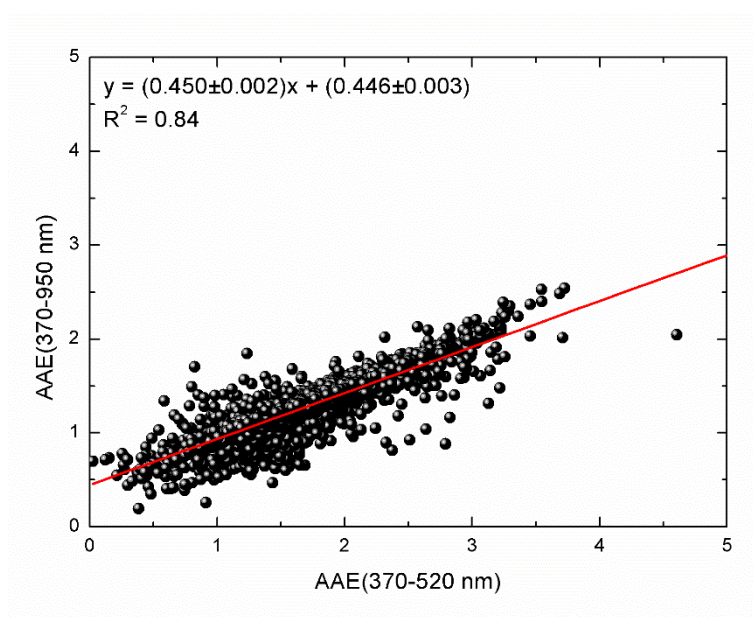
SUPPLEMENTARY MATERIAL

Figure S1: Scatterplot of AAE(370-520 nm) and AAE(370-950 nm) at UGR station for the period Sept 2012 – Sept 2015.
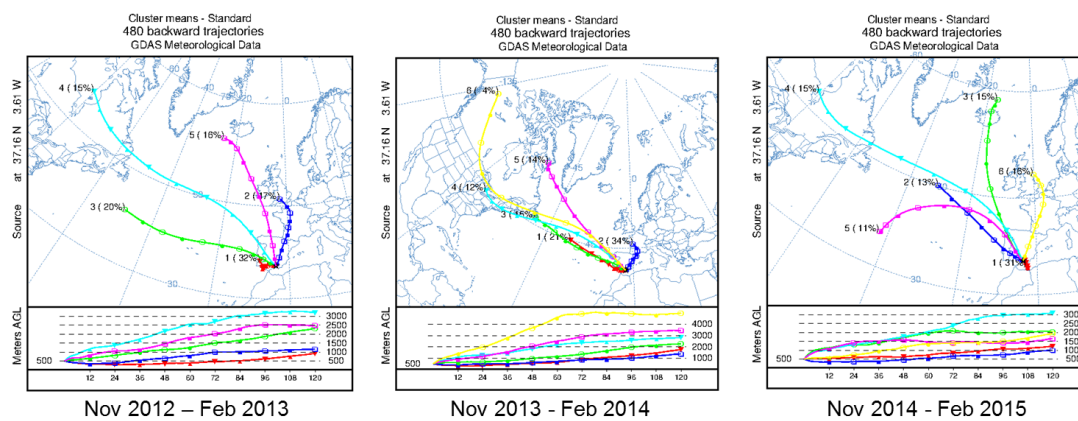

Figure S2: Cluster analysis of 5 days air mass back-trajectories arriving at Granada at 500 m asl for the periods November 2012 – February 2013, November 2013 - February 2014 and November 2014 – February 2015.
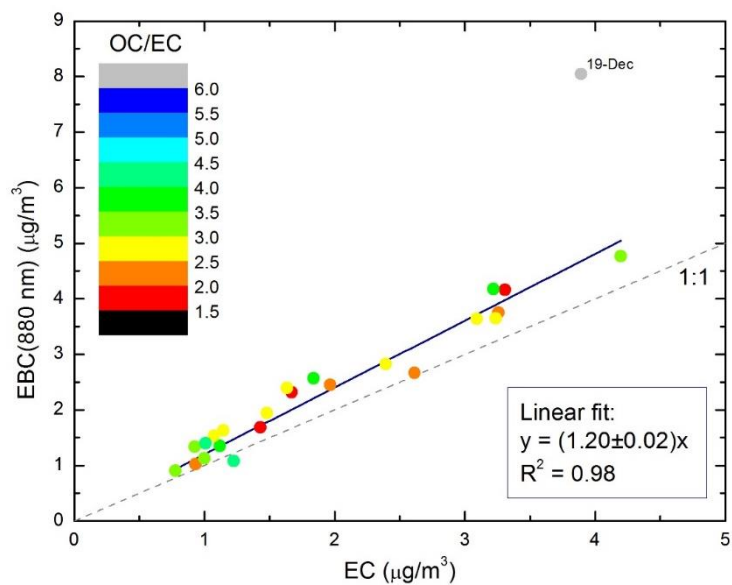
Figure S3: EBC mass concentration determined with the Aethalometer versus EC mass concentration from filter samples with 24-h time resolution analyzed with the EUSAAR2 protocol for the period September 2012 – September 2013. The color scale indicates the OC/EC ratio. The linear fit calculated excluding the 19 December 2012 sample and the 1:1 line are included.